

Article

# Design of Experiments Technique Applied to Artificial Neural Network Models for FPSO Mooring System Analysis

Ehsan Nikkhah \* , Antonio Carlos Fernandes  and Jean-David Caprace 

COPPE, Federal University of Rio de Janeiro (UFRJ), Rio de Janeiro 21941-853, Brazil;  
acfernandes@oceanica.ufrj.br (A.C.F.); jdcaprace@oceanica.ufrj.br (J.-D.C.)

\* Correspondence: ehsan.nikkhah.ir@oceanica.ufrj.br; Tel.: +55-219-9175-1940

**Abstract:** Online monitoring of mooring system response for the FPSO platform in any operational condition is so far challenging for machine learning (ML). This paper presents a new dynamic NARX ANN model for time series of mooring tension and a static MLP model for the offset chart prediction of a taut-leg moored FPSO with different working scenarios. A novel method for supervised feature selection of the dataset was applied to determine the most influential design features. Additionally, a design of experiments (DOE) technique was implemented for test matrix creation, simulation, database generation, and supervised selection characteristics in ML. The DOE analysis revealed that the mooring configuration, platform loading condition, and environmental loads alter the platform's six-degree-of-freedom motion response patterns. These input data were used to predict the mooring tension and the offset chart of the floater. The results include the fair values of statistical error for mooring tension ( $R^2 = 0.8\text{--}0.98$ ,  $E \approx 1.3\text{--}5.7\%$ ,  $RMSE \approx 6\text{--}66$  kN) and platform offset ( $E \approx 0.1\text{--}1$  m) prediction when testing the trained models with unseen data representing new operational conditions. Faster convergence can be achieved by adding non-numeric (string) input values to dataset numeric features. Supervised feature selection of the dataset is a step forward in ML to improve prediction accuracy.

**Keywords:** artificial neural network (ANN); supervised feature selection; deep learning; design of experiments (DOE); mooring system response prediction; FPSO platform



**Citation:** Nikkhah, E.; Fernandes, A.C.; Caprace, J.-D. Design of Experiments Technique Applied to Artificial Neural Network Models for FPSO Mooring System Analysis. *J. Mar. Sci. Eng.* **2023**, *11*, 2194. <https://doi.org/10.3390/jmse11112194>

Academic Editors: Spyros A. Mavrakos and Decheng Wan

Received: 12 October 2023  
Revised: 25 October 2023  
Accepted: 11 November 2023  
Published: 17 November 2023



**Copyright:** © 2023 by the authors. Licensee MDPI, Basel, Switzerland. This article is an open access article distributed under the terms and conditions of the Creative Commons Attribution (CC BY) license (<https://creativecommons.org/licenses/by/4.0/>).

## 1. Introduction

FPSO platforms are used extensively by the offshore oil and gas industry and have become one of the primary methods of oil and gas processing, storage, and offloading. Due to the operational requirements of the offshore oil fields, the FPSO platform and its mooring system must comply with the site specification in terms of depth, subsea layout, sea state intensity, production, and offloading capacity. The mooring layout that includes the anchorage radius and the line azimuth inclination angle might be changed to adapt to new subsea layouts. Production and offloading capacity require different loading conditions, demanding adaptation to pre-tensions in mooring clusters. Therefore, an FPSO platform confronting different operational obligations requires loading and mooring adjustments. As illustrated in Figure 1, an FPSO anchor mooring line in deep water is multi-segmented and usually comprises more than one material that spreads in a taut-leg profile around the floater. The practical solution in deep offshore operations is the chain–polyester–chain technology, which provides, via segmentation, greater stiffness and a higher strength-to-weight ratio [1]. The taut leg mooring system responds to the floater's movements through line tensions created by elastic stiffness  $K_E$ , derived from the elastic properties of the polyester segment of the mooring line. Many mooring systems are fitted with inclinometers designed to report line tensions. An inclinometer measures the angle of inclination of a mooring line. These systems can calculate the tension force based on

the top angle reference ( $\alpha$ ), the total length of the anchor mooring line laid in the taut leg profile ( $l$ ), and the strain ( $\Delta\epsilon$ ) to elastic stiffness Equation (1)

$$K_E = EA \frac{1}{l} \sin \alpha \Delta F = K_E \Delta \epsilon \tag{1}$$

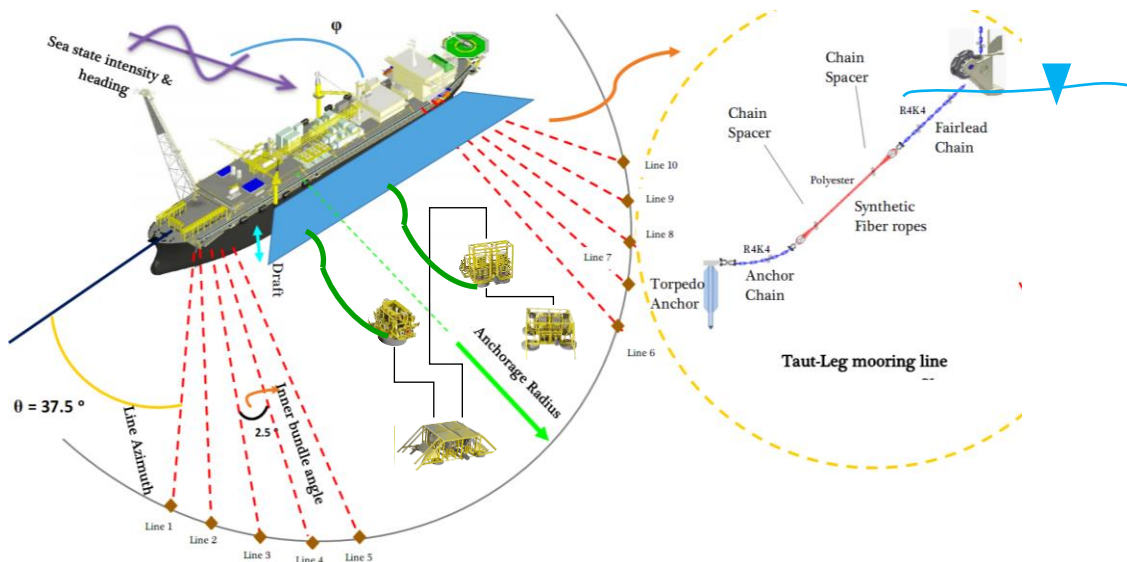


**Figure 1.** Taut-leg moored FPSO with twenty mooring lines.

The instrumentation components are often fully exposed to the seawater and harsh environment in which the mooring lines are located. Water ingress, corrosion, cable connections, acoustics, and battery life are some of the issues that have caused system malfunctions. Some inclinometer systems had poor reliability records, generating false readings and out-of-work situations [2].

The mooring tensions and the floater’s offsets are highly correlated with the platform response to environmental loads. It is known that the platform offset allowable limit (eight percent of water depth) is a valuable reference for securing the target offshore site and the uninterrupted watchkeeping of mooring line tension, which is vital for station-keeping, operability, and integrity management of offshore floating platforms. In view of that, ML surrogate models can be a virtual alternative to predict tension time series on mooring lines and offset charts. The design of experiments (DOE) technique was employed to investigate the most influential design variables affecting the mooring line tension and platform offset to provide optimum feature selection for the artificial neural network (ANN) dataset.

In this article, supervised learning was applied to predict relevant statistics, such as anchor mooring tension and offset charts associated with any operational conditions that the FPSO platform might face under dynamic response to generic environmental loads. ANN models were trained and tested through data obtained from the numerical simulation of a dynamic model. However, for real cases, the data can be obtained through long-term monitoring and observation of live platform sensors in operation. These include the Differential Global Positioning System (DGPS) and Motion Reference Units (MRUs) for the six-degree-of-freedom motions, Draught Measuring Sensor (DMS) for loading draft, Mooring Observatory Sensors (MOS) for mooring lengths and layouts, and Automated Identification System (AIS) for the exact position of platform in the offshore field. Then, ANN surrogate models can be taken onboard the original FPSO prototype to perform tension prediction, feeding the dataset with the online data acquired by the mentioned sensors. The whole concept of the proposed method, from data acquisition to user interaction, is illustrated in Figure 2.

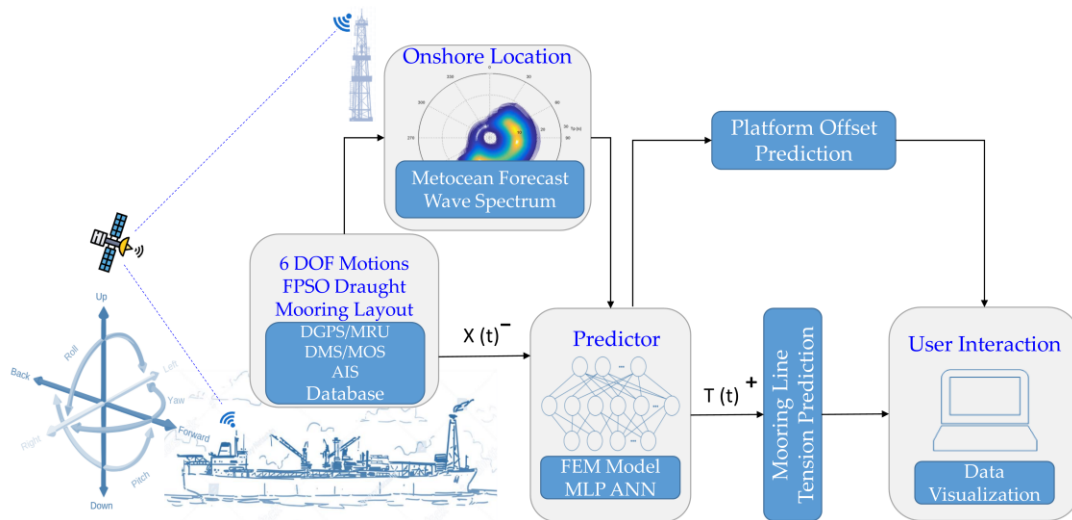


**Figure 2.** System diagram of online mooring tension prediction and floater's offset chart. DGPS: Differential Global Positioning Systems; MRU: Motion Reference Unit; DMS: Draught Measurement system; MOS: Mooring Observatory Sensors; AIS: Automated Identification System.

There is a need for long-term response prediction of mooring systems via ML techniques. ANN is the most effective and widely used ML method for deep learning dynamics of highly complex non-linear problems, such as mooring line tension and floating platform offset prediction [3]. Over the past few decades, this approach has been particularly successful compared to analytical hydrodynamic models. Simoes et al. (2002) proposed a neural network architecture to predict the top tension on mooring lines and a hawser in a system where a turret-FPSO is connected to a shuttle tanker by the hawser. The model performed a faster simulation by replacing a huge amount of numerical calculations to represent an actual system's dynamic behavior [4]. Guarize et al. (2007) trained an ANN using the original short time series response (500 s) of slender structures, simulated via a finite element method (FEM) approach, to obtain a longer time series (10,800 s), reducing its computational cost. The hybrid ANN approach has been verified to be accurate in predicting a structural response with low non-linearity. However, due to the short input period of time, in terms of strong non-linearity, it lacks in precision [5]. Christiansen et al. (2013) implemented a hybrid FEM-based method using six-degree-of-freedom platform motions and delayed time steps as the input for training an ANN. The resultant mooring restoring force was predicted in different sea states for fatigue analysis. This methodology was accurate enough for fatigue estimation of slender structures [6]. Similarly, de Pina et al. (2013) proposed an ANN associated with a NARX model that can obtain the response of a floating production and storage platform (FPS). The model showed good agreement with the results provided via FEM based non-linear dynamic analysis [7]. Afterward, de Pina et al. (2014) proposed surrogate meta-models with an approach based on wavelet networks (WN), a combination of a feedforward neural network architecture with the wavelet transform method to obtain dramatic reductions in processing time, while providing results nearly as good as those of non-linear dynamic FE methods [8]. Finally, de Pina et al. (2016) presented the development of ANNs to analyze any arbitrarily defined spread-mooring configuration for semisubmersible FPS [9]. Sidarta et al. (2017) proposed an ANN-based mooring line top tension prediction system that receives semisubmersible platform six-degree-of-freedom motions with lag time histories as the input. The paper compares time series of mooring line tensions for sea states that were and were not included in training [10]. Yetkin et al. (2017) and Yetkin and Kim (2019) proposed mooring top tension prediction systems based on a NARX neural network for a faster simulation by predicting tension time histories under unseen environmental conditions [11]. Dong et al. (2020) proposed a methodology to assess the reliability of mooring lines under extreme environmental

conditions based on ANN–Bayesian network inference. Different types of ANN, including neural networks of the radial basis function and neural networks of backpropagation, were adopted to predict the extreme response of anchor lines according to a series of measured environmental data [12]. Zhao et al. (2021) presented a hybrid FEM BP ANN model to more conveniently predict the statistic pre-tension and dynamic tension time series with several design variables related to mooring systems under irregular sea states. Statistical error evaluation has proven the precision of this approach [13]. Lee et al. (2022) used a standardization technique in building an ANN-based mooring line top tension prediction system, proving that batch normalization (BN) and learning rate decrease (LRD) improve the prediction performance [14]. Cotrim et al. (2022) proposed a set of data-based surrogate models with environmental data as input. Each model specialized in predicting motion statistics relevant to the design of mooring systems: maximum roll, platform offset, and fairlead displacements. It was concluded that an ANN surrogate model could be trained directly, using actual measured metocean conditions and the corresponding FPSO motion statistics, providing greater accuracy and reduced computational time over traditional methods based on dynamic simulation [15]. Peng Li et al. (2022) proposed an ANN model based on long short-term memory (LSTM) for tension prediction of an FPSO single-point mooring system with satisfactory results [16].

From most of mentioned research, a common approach can be seen. The input had only numeric values with either a combination of metocean data or the floater's response. The main contribution of the current work is to add non-numeric and numeric features to the dataset representing all possible working scenarios of an offshore floating unit. These include the sea state measurements, mooring system configuration, operational condition, and dynamic response of the platform. Specifically for mooring tension prediction, platform loading conditions (draft), and mooring layout (number of anchor lines, length, azimuth) are introduced as non-numeric input values, and the floater response (6DOF) is considered as a numeric input feature, to the NARX model. Input attributes to the static MLP for the prediction of platform offset are a combination of non-numeric and numeric figures, including metocean data and platform loading condition. Furthermore, compared to similar research, the proposed framework presents supervised feature selection of the dataset. The work highlights that input features with non-numeric (string) and numeric values lead to faster convergence of the target output. A massive database develops and validates two distinguished data-driven static MLP and dynamic NARX models. They were trained and tested on 3,446,077 sample cases for tension time series and 13,320 sample cases for offset chart prediction.

## 2. Methodology

The steps to achieve the main goal are summarized in Figure 3. The procedure consists of three main modules: numerical modeling of the case study; test matrix definition and simulation; and database generation with ANN deep learning. Initially, the procedure started with modeling the case study FPSO platform with a mooring system operating in the target offshore field. It includes all structural parameters, settings, and geometrical configurations. The numerical model must be as close as possible to the prototype for higher simulation accuracy. These include considering similarities between hydrostatic features, hydrodynamic coefficients (added mass, damping), and eigen periods (natural frequencies) of the total system that arise from the platform and the connected mooring–riser system.

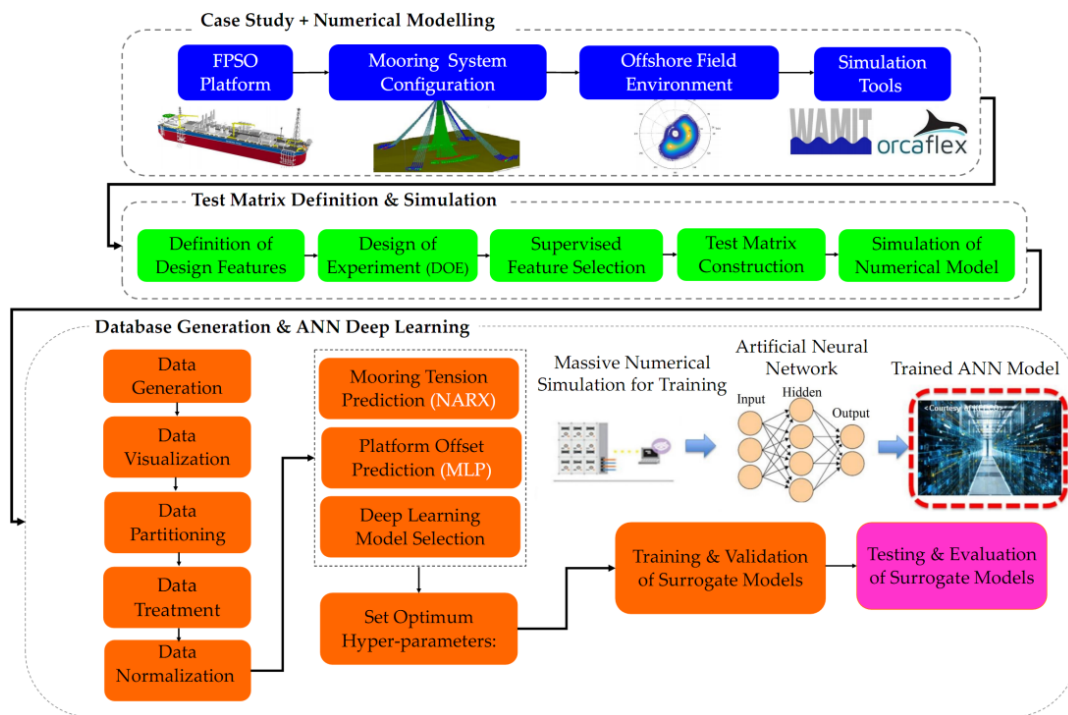


**Figure 3.** The design process for mooring system response prediction of FPSO platform.

Determination of the environment metocean data of the offshore site and simulation tools for the whole model are also considered in this stage. The next step is to define a test matrix that simulates the platform’s working scenarios. It requires considering input design variables whose magnitudes influence the output response. These design features (design factors) are attributed to platform loading conditions, mooring system configurations, and metocean data of the offshore field environment. The outputs response are mooring line tension time series and platform offset. The design of experiments technique is employed to understand the relationship between the input design factors and output response. Factorial analysis evaluates the effect of each input feature on the output response. This process, called supervised feature selection, identifies the most effective input parameters affecting the output response. It is assumed that the test matrix created by low and high levels of these selected input features will epitomize the platform’s operational conditions. Simulation of the numerical model according to test matrix run orders is performed to obtain mooring line tension time series and platform offset. At the last step of the research methodology, the dataset generated by 3 h simulation is visualized, prepared, and split into training, validation, and testing subsets. After selecting the proper ANN model related to each problem, the settings of hyperparameters will be performed. Finally, the ANN models are trained, tested, and evaluated against metric errors.

### 3. Case Study

In this work, an FPSO with 2 MBBLs capacity was used as an initial model. The main particulars of the FPSO model are listed in Table 1. The IS rule (IMO, 2008) and IMO MODU rule (IMO, 2009) were applied to check the intact stability of the given FPSO through hydrostatic analysis. The mass and hydrostatic stiffness of the FPSO for full and ballast loading conditions were obtained, which were the required ones for the hydrodynamic analysis. The main purpose of the hydrodynamic analysis is to establish response amplitude operators (RAOs) for the motion and relative waves for the interested points. Here, the RAO is a transfer function defined as the complex amplitude of a response to an incident wave of unit amplitude, frequency  $\omega$ , and direction  $\theta$  (Newman, 1977). To obtain the RAOs of the motion and relative waves, added mass, radiation damping, wave excitation, and elevation, a commercial software was used. The motion analysis was carried out for full

and ballast drafts. The wave frequency range used for motion analysis is from 0.2 rad/s to 1.2 rad/s at 0.03 rad/s intervals, for a total of 35 frequencies, and wave directions from 0° to 180° at 22.5° intervals. For seakeeping analysis, the noticeable model test results mentioned in Lopez et al., 2015, were compared and validated, considering the numerical results of both translational (surge, sway, heave) and rotational (roll, pitch, yaw) motions of FPSO at different wave directions [17]. The taut-leg spread mooring system, designed to ensure safety through station keeping, consists of 20 mooring lines in four clusters, each one comprising 5 mooring lines arranged at 2.5° intervals, as illustrated in Figure 4. The layout and specifications of the mooring system are detailed in Table 2. Fairleads positions of the mooring lines are, in relation to the FPSO center, oriented positive to bow and to portside, and their azimuths are in the direction of where the line is facing, counterclockwise to the vessel's north. The final numerical model was constructed by Orcaflex® 11.0b for fully coupled dynamic time domain analysis. The adjusted JONSWAP wave spectrum was used for wave simulation that implements irregular waves in the Santos basin in Brazil. Numerical free decay tests of the taut-leg moored FPSO in still water were also carried out for the six-degree-of-freedom motions to calculate the eigen periods. The natural periods of the total system are listed in Table 3 and depicted in Figure 5. The differences for all six-degree-of-freedom (DOF) motions between the numerical model and the prototype, for both low frequency (surge, sway, yaw) and wave frequency response (heave, roll, pitch), are within 5% deviation from the reference values proposed by the DNV-GL and acquired by the actual prototype FPSO [18,19].

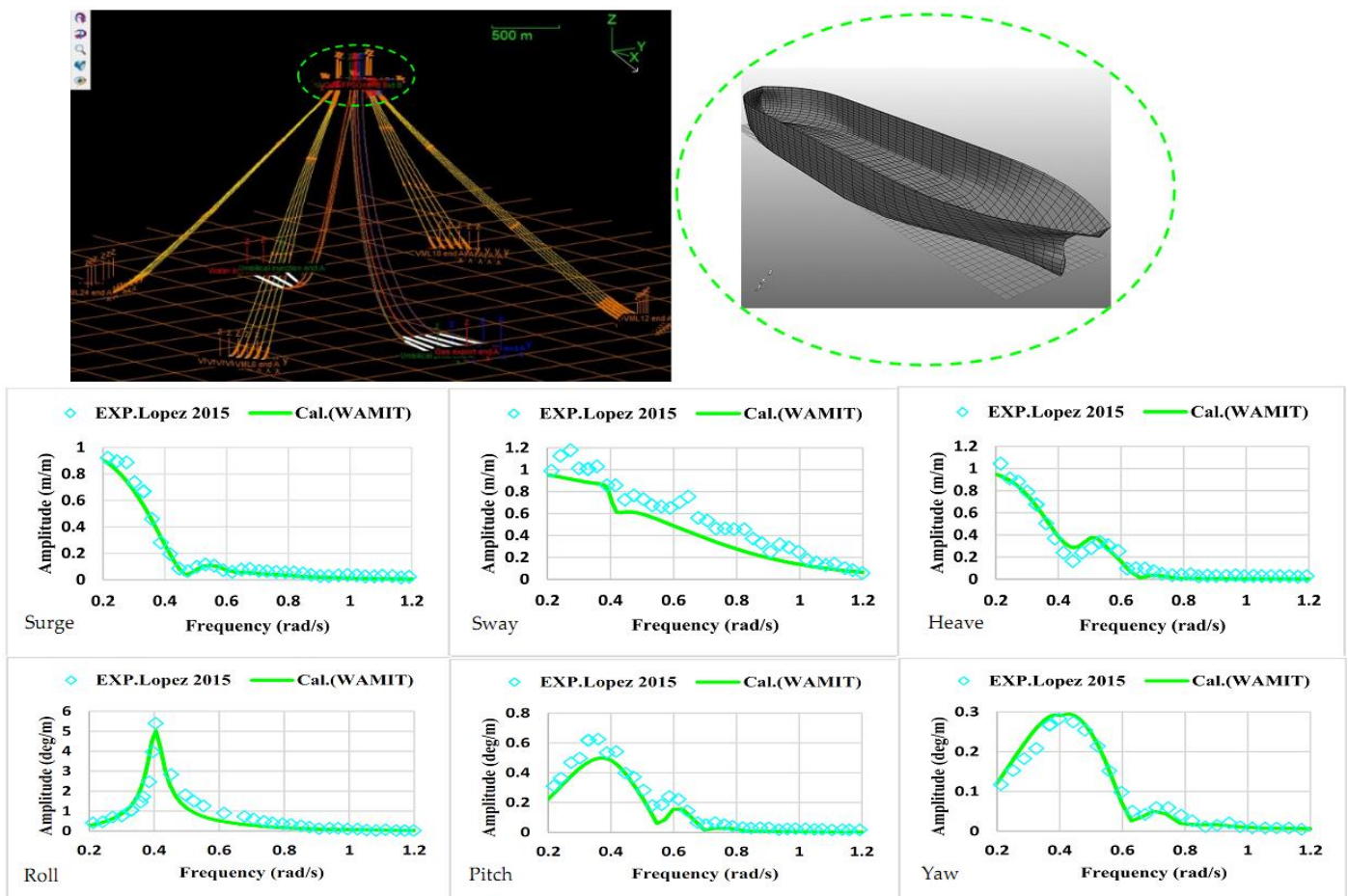


Figure 4. Numerical model and validation of RAO through hydrodynamic motion seakeeping analysis of FPSO at full draft [17].

**Table 1.** Main details of case study FPSO [19].

Description	Loaded Condition	Ballast Condition
Length overall	337.35 m	337.35 m
Length B.P.	320 m	300 m
Breath	54.6 m	54.6 m
Depth	27.8 m	27.8 m
Ship draught	21 m	11 m
Longitudinal center of gravity	144 m	152 m
Vertical center of gravity	16.7 m	19.5 m
Mass radius of gyration in x axis	16 m	15 m
Mass radius of gyration in y axis	80 m	75 m
Mass radius of gyration in z axis	80 m	75 m
Operating Water Depth	1500 m	1500 m

**Table 2.** Layout of fairleads and anchor lines properties [19].

Line N°	X (m)	Y (m)	Z (m)	Azimuth (degree)	Description	Magnitude		
1	146	24	19	37.5	Number of lines	4 × 5		
2	142	25	19	40	Outer bundle angle	37.5°		
3	138	26	19	42.5	Inner bundle angle	2.5°		
4	134	27	19	45	Anchor radius	2500 m		
5	130	28	19	47.5	Segment (No)	Ø <sub>nom</sub> (mm)	Material	Weight in water (kN/m)
6	−116	28	19	132.5	1	114	R4K4 Chain	2.238
7	−120	27	19	135	2	225	Polyester	0.086
8	−124	26	19	137.5	3	114	R4K4 Chain	2.238
9	−128	25	19	140	4	225	Polyester	0.086
10	−132	24	19	142.5	5	114	R4K4 Chain	2.238
11	−132	−24	19	217.5	6	225	Polyester	0.086
12	−128	−25	19	220	7	120	R4K4 Chain	2.48
13	−124	−26	19	222.5	Segment (No)	EA <sup>1</sup> (kN)	Length (m)	MBL <sup>2</sup> (kN)
14	−120	−27	19	225	1	919,077	350	12,420.4
15	−116	−28	19	227.5	2	206,010	900	13,734
16	130	−28	19	312.5	3	919,077	10	12,420.4
17	134	−27	19	315	4	206,010	900	13,734
18	138	−26	19	317.5	5	919,077	10	12,420.4
19	142	−25	19	320	6	206,010	500	13,734
20	146	−24	19	322.5	7	982,080	200	13,573

<sup>1</sup> Axial stiffness. <sup>2</sup> The chain minimum break load (MBL) presented is the value without corrosion.

**Table 3.** Natural periods<sup>1</sup> of FPSO with taut-leg mooring system operating in deep water [18,19].

	Surge	Sway	Heave	Roll	Pitch	Yaw
DNV-GL FPSO	>100 (S)	>100 (S)	5–12 (S)	5–30 (S)	5–12 (S)	>100 (S)
Original FPSO	265 (S)	225 (S)	11 (S)	14 (S)	10 (S)	155 (S)
Numerical Model	250 (S)	212 (S)	12 (S)	14 (S)	10 (S)	150 (S)

<sup>1</sup> The number of mooring lines involved in the mooring operation and the water depth influence these values.

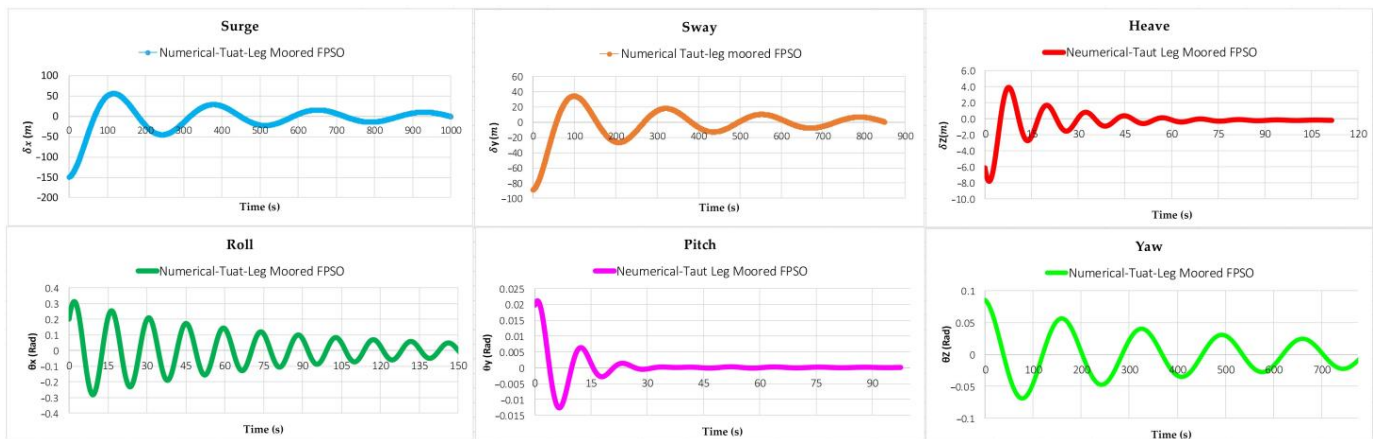


**Figure 5.** Natural periods of the system determined by the numerical free decay test in 6DOF at full draft condition.

#### 4. Design of Experiments (DOE) for Supervised Feature Selection of Dataset

The design of experiments (DOE) technique is defined to evaluate the factors that affect the value of an output parameter or a group of parameters. DOE is usually employed when more than one input factor is suspected of influencing an output. By varying multiple inputs simultaneously, DOE can identify important interactions that may be missed when experimenting with one factor at a time. For this purpose, all possible combinations of factors can be investigated. The design matrix will show all the possible combinations of high and low levels for each input factor. A two-high–low-level design with  $k$  factors requires a minimum of  $2^k$  test runs to accommodate all possible combinations of factor levels in a full factorial design [20]. This work's response, or variable of interest, is the platform offset and the tension force induced in the mooring line. Although both are mutually correlated to each other, the interaction between the platform offset and mooring system response is completely non-linear. It depends on vessel operational conditions and mooring system design features, which vary in every offshore location. Environmental loads bring about a non-linear motion response in the platform, resulting in the mooring system reaction according to mass, damping, and stiffness of the total system. System response varies with the depth, intensity, and heading of the approaching sea state, number of anchor lines, mooring line properties and components, the anchorage radius, the azimuthal inclination angle of the line, the pre-tension in operation, and the draft of the floating platform due to varying loading conditions. These are the main parameters for precisely predicting the dynamic behavior of the mooring lines and floating platform. The excitations of the sea environment (wave, wind, current), as shown in Figure 6, lead to platform offset and tremendous tension on mooring lines. Considering the role of environmental load on the non-linearity between offset and line tension, the contribution of wind and current is much lower than the contribution of the wave, as illustrated in Figure 6. This is the main reason why wave-only simulations are considered in this study to capture the non-linear behavior between dynamic platform motions and their corresponding line tension response using artificial neural networks. However, the offset and mooring line tension will be obtained through fully coupled time domain simulation of the dynamic model under predefined environmental and operational conditions.

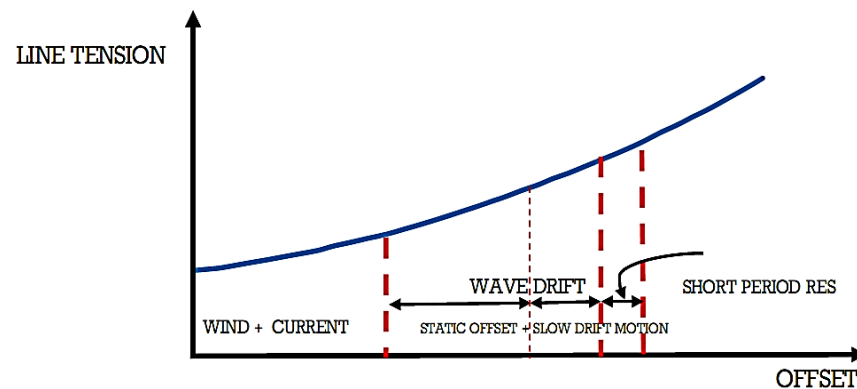


**Figure 6.** Typical non-linear offset v/s line forces (tensions) [21].

Feature selection in machine learning (ML) is the method of reducing the input variables to a specific model by using only relevant data and eliminating useless data with low effectiveness that are considered noise in data. Supervised feature selection refers to the method that uses the output variable to assess the effectiveness of the input variables for selecting the features of the dataset. The target variable will be used to identify the input variables that influence the output, which can increase the model's efficiency. Design of experiments (DOE) is an effective tool employed to introduce a supervised feature selection technique for analyzing mixed-attribute data capable of evaluating each attribute's effectiveness on the target value in the dataset. Since the ANN is a tool for pattern recognition, it can, in principle, only predict patterns similar to those used for training the network. Due to the need for many time series realizations with different conditions, the ANN must be trained to cover a broad range of predefined features. Features are the basic building blocks of datasets. The quality of features in the dataset has a major impact when it is used for deep learning. This means that the training dataset must be selected such that all extremes are included, and enough data between the extremes are also considered to secure a satisfactory representation of different levels of the non-linear behavior. The specified attributes and their upper and lower limits used for the design of the experiment analysis and, subsequently, the supervised selection of the dataset for ANN are illustrated in Table 4. Note that the sea state with  $H_s = 16$  and  $T_p = 17$  is not part of the test dataset as it was not part of the original wave scatter diagram. This sea state is merely included for a training dataset to stretch the range of extremes in the ANN to improve the accuracy for the largest relevant wave heights.

DOE test runs carry out experiments to determine how affected is the output in terms of the many considered attributes. It is based on factorial analysis. The ANN dataset's target values of interest are platform offset and mooring tension. After accomplishing the DOE factorial analysis based on defined attributes (Table 4), the main effect plots and Pareto charts are depicted in Figures 7 and 8, respectively. As can be seen, according to the supervised feature selection technique, only draft (B), sea state (E), and heading direction (F) are chosen as features for training, validation, and testing of the dataset for platform offset prediction. On the other hand, all attributes, including number of mooring lines (A), draft (B), anchorage radius (C), azimuth inclination angle (D), sea state condition (E), and heading direction (F) influence the mooring tension and shall be taken as dataset features for training, testing, and validation. It should be noted that instead of sea state and heading direction, its immediate response (the six-degree-of-freedom platform motions), which are easily measured by ship sensors (DGPS and MRUs), are taken for the prediction of mooring tension.

**Table 4.** Upper and lower limits of the mooring and operational design variables used for dataset features determination of ANN dataset features. (Training data are marked by orange color ‘O’, and testing data are marked by blue color ‘□’.)

Attributes	Level Low -1		Level High +1		Test Runs						
Number of lines	20		28		20, 28	2					
FPSO draft (m)	11		21		11, 14, 16, 21	2					
Anchorage Radius (m)	2500		3000		2500, 2750, 3000	2					
Line Azimuth Angle (°)	2.5		5		2.5°, 3.5°, 5°	2					
Line Pre-tension (kN)	Cluster NW	1950	Combination 1	1850	Combination 2	2					
	Cluster SW	1750		1650							
	Cluster NE	2000		1900							
	Cluster SE	2050		1950							
Santos Basin Offshore Brazil Wave Scatter Diagram [22]											
Sea State ( $H_s/T_p$ ) (m/S)	3	5	7	9	11	13	15	17	19	21	
2	X	X	O	X	X	X	X	X	X	X	8
4		O	X	X	X	□	X	X	O		
6			X	□	O	X	□	X			
8				X	X	O	X	□			
10					□	X	X	O			
12						□	O				
16								O			
Sea State Heading (°)	N		NE	E	SE	S	SW	W	NW		8
	180°		135°	90°	45°	0°	315°	270°	225°		

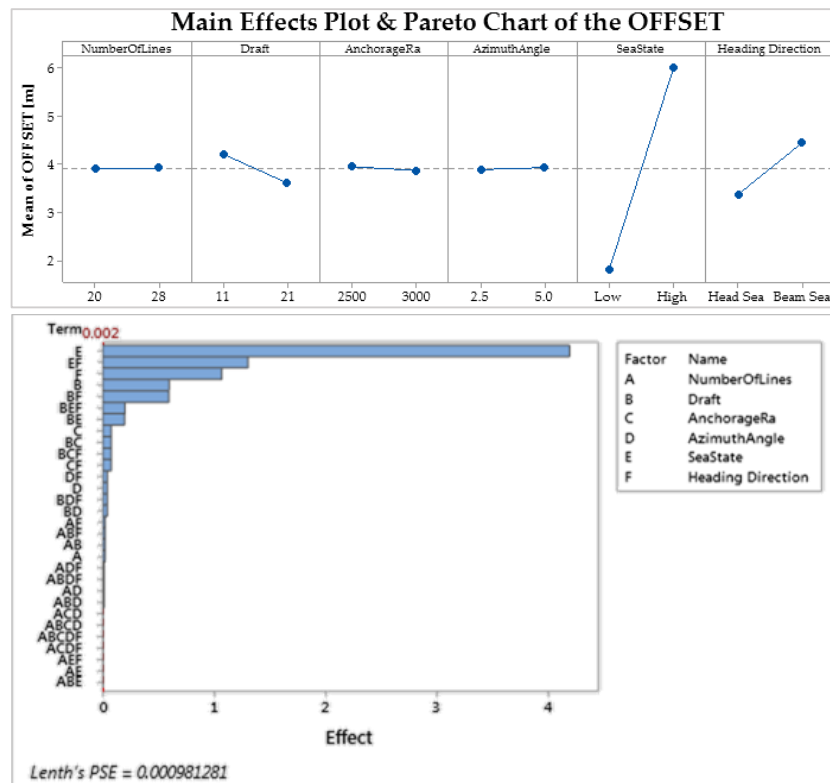


**Figure 7.** Factorial analysis of design variables and their effects on floater’s offset.

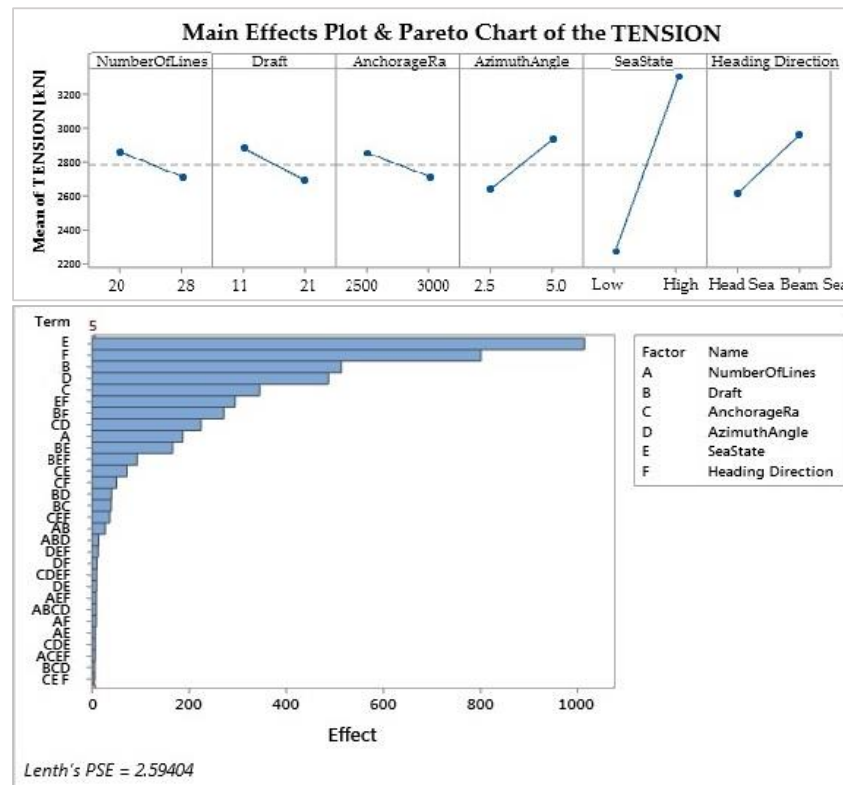


Figure 8. Factorial analysis of design variables and their effects on mooring line tension.

## 5. Machine Learning

### 5.1. Deep Learning

Deep learning was first introduced to ANNs by Aizenberg et al. (2000), and subsequently, it became especially popular in the context of deep NNs [23]. Deep learning is a class of machine learning algorithms that uses multiple layers to progressively extract complex and higher-level features from the raw input. The output of one layer becomes an input to the next processing layer, creating a deep architecture [24]. Proper use of deep learning model requires a correct understanding of solving strategies for specific problems. The prediction of mooring line tension time series demands a time-dependent dynamic network, while the prediction of the platform offset needs a finite static model. Both static and dynamic models can be embedded in two distinctive MLP deep feedforward ANN with backpropagation as the quintessential deep learning models. A non-linear autoregressive exogenous network (NARX) is a complex discrete-time non-linear system with feedback connections that was first explained by Menezes and Barreto et al., 2008 [25]. This model is usually applied to the long-term (multistep-ahead) prediction of univariate time series such as mooring line tension. For time series modeling, NARX utilizes current and past values together with non-linear input–output mapping for dynamical prediction. Each neuron uses a non-linear activation function to perform a scalar product operation. A high-level open source API wrapper from a Python library that covers every step of the machine learning workflow, from data processing for datasets featuring string and numeric values to hyperparameter tuning, was used for deep learning [26]. The proposed deep artificial neural network model for tension prediction time series is illustrated in Figure 9.

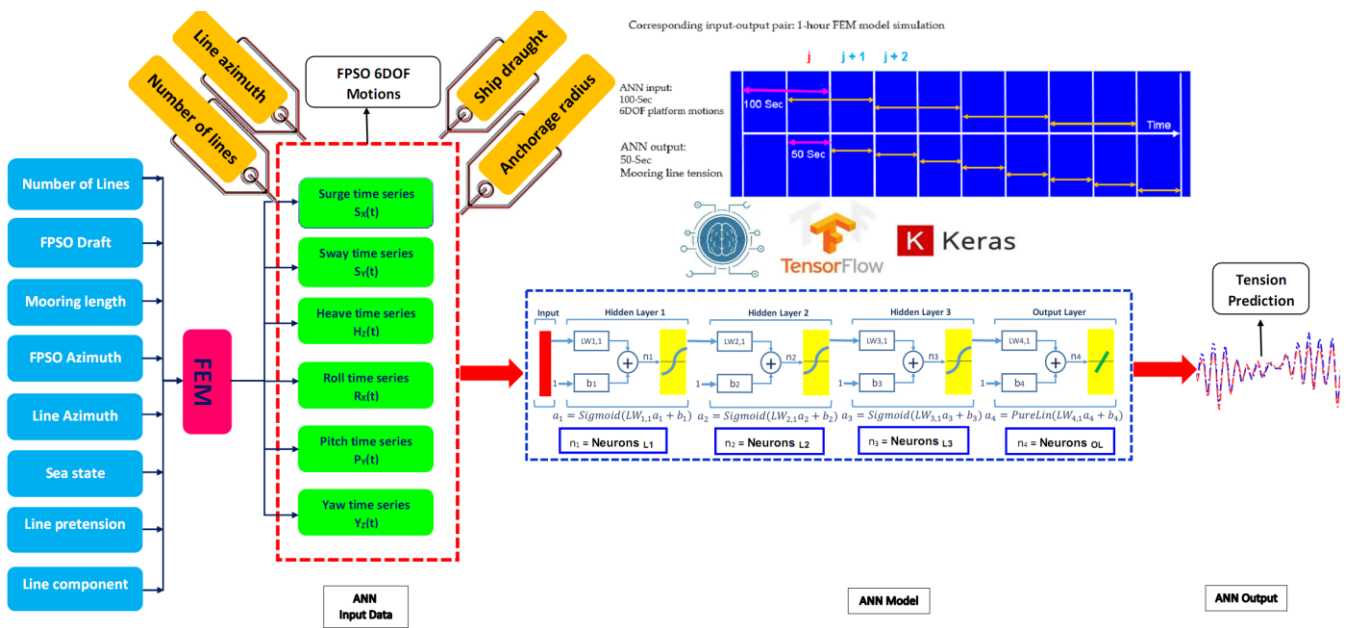


Figure 9. Structure of non-linear autoregressive exogenous MLP BP DFF NNs with input features, output, and three hidden layers.

5.2. Hyperparameter Optimisation

Hyperparameters in ML are those that control the learning process. These include the number of hidden layers and number of neurons in each layer, activation function, loss function, number of epochs, batch size, and the optimizer with appropriate learning rate decay (LRD) that provides an apparent improvement in the prediction performance. ANN hyperparameter optimization consists of determining the optimal hyperparameters for a given task [27]. Finding the optimal hyperparameters for an ANN model has always been an essential yet demanding and time-consuming task, which is performed via trial and error, requiring a lot of experience with ANN training. In order to use gradient methods to optimize the model, the activation function has to be continuous, with a finite range that has a more stable performance and is typically symmetric around the origin. The most common activation function for regression neural networks is the Sigmoid function, which is continuous, has a finite range, and is symmetric around the origin. The Sigmoid function is defined as shown in Equation (2) and Figure 10, including the function’s derivative.

$$f(z) = \frac{1}{1 + e^{-z}}, f'(z) = \frac{1}{1 + e^{-z}} \cdot \left(1 - \frac{1}{1 + e^{-z}}\right) \tag{2}$$

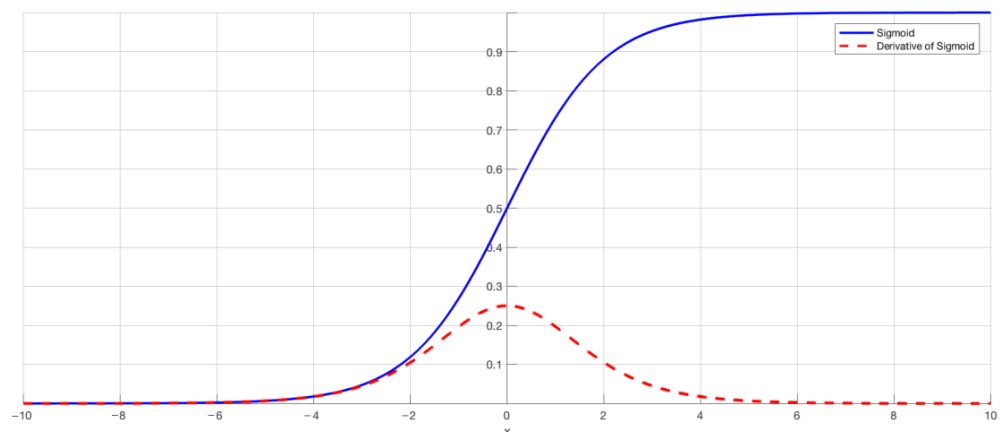


Figure 10. Logistics activation function [27].

When the network has given an output, it is compared with the target value. A loss function gives a value for how well the network has performed. This loss function calculates the error of the regression problem. The mean square error (MSE) is defined as shown in Equation (3), used because the error function is so far very convenient and usually leads to good ANN performance. This loss function weighs larger errors more heavily than any other cost function. Consider that  $y_i$  is the output,  $\hat{y}_i$  is the target value, and  $N$  is the number of data points.

$$L(y, \hat{y}) = \frac{1}{N} \sum_{i=0}^n (y_i - \hat{y}_i)^2 \tag{3}$$

Setting the optimal number of epochs is of great importance as well. Too few epochs will not train the model sufficiently, and too many epochs will overtrain the model. As the number of epochs increases, the same number of times weights are changed in the neural network, and the boundary goes from underfitting to optimal, then to overfitting. Underfitting happens when insufficient training results in poor performance on the training data and poor generalization to other data. Generalization is a term used to describe a model’s ability to react to new data and make accurate predictions. On the other hand, overfitting occurs when, due to overtraining, the model’s good performance only appears in the training data, but a poor generalization still exists in other data. The training process of a neural network is an iterative process where an epoch is an iteration of the whole training dataset. The input data to the neural network are split into training, testing, and validation datasets. The training data are read by the model and used to change the weight of the neurons and consequently train the model. In each epoch iteration of the training, a small dataset called validation data is used to validate the accuracy of the weights in the epoch. This is performed to track the development of the model accuracy during the learning process. When the model is fully trained on the training data, the model is tested against the third dataset split, which is the testing dataset. It is important for the neural network to be tested against data in which the model has never been exposed before. Therefore, the original dataset is divided into training, validation, and testing, as illustrated in Figure 11.

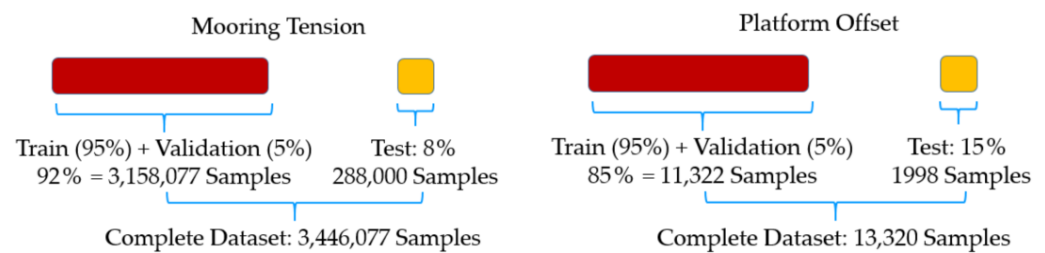


Figure 11. Dataset allocations for training, testing, and validation.

The optimization algorithms use the loss function to optimize the weights in the neural network. Minimizing the loss, calculated with the loss function, the error is consequently minimized. The common and the most used optimization algorithm leading to faster convergence is the Adam optimizer implemented in the training of dataset. The process of successfully creating and training ANNs to solve a domain-specific task highly depends on its hyperparameter tuning. The optimization skill of the meta-model, which would typically be various, is gained from repetitive trying and failing of ANN modeling and domain knowledge from previous experiences. The hyperparameters of the ANN meta-models of the current study for the prediction of mooring tension and platform offset are illustrated in Table 5. As can be seen, except for the number of neurons in each layer and the activation function between hidden layers, all other hyperparameters are the same. A larger network structure for the dynamic NARX model is indispensable for deep learning, considering the time correlation and complex dynamics of mooring tension, while for

the static MLP, the network structure shall not be computationally expensive. Thus, the ReLU activation function, which is more computationally efficient when compared to the Sigmoid, has been selected. The training process halts when the validation error stops decreasing or even increases to prevent ANNs from over-fitting. The Keras® early stopping method that uses the training and validation sets to keep track of network performance was implemented. The training process is stopped when the model stops improving on a validation set. After training, the predictor model predicts the target output in a testing phase. The testing dataset feeds the trained executor model, and the test units must have the same dimensions defined for the training units; i.e., the same input and output sizes must be used in the training and test phases. The test data were extracted from a numerical model according to the defined attributes of the new operational conditions that a floating platform might face. Data generated for testing were completely different from those used for training and unseen by the trained model to observe its performance.

**Table 5.** Hyperparameters of ANN meta-model.

Parameter	Mooring Tension	Platform Offset
The number of hidden layers	3	3
The number of neurons in each layer	611, 3 × 1222, 50	6, 18, 24, 18, 1
Activation function between hidden layers	Sigmoid	ReLU
Activation function before output layer	Linear	Linear
Loss function	MSE	MSE
Batch size	100	100
The number of epochs	100	100
Optimizer	Adam	Adam
Learning Rate	0.001	0.001
$\beta_1$	0.9	0.9
$\beta_2$	0.999	0.999
$\epsilon$	$1.0 \times 10^{-8}$	$1.0 \times 10^{-8}$
Learning Rate Decay	0.0	0.0

5.3. Error Fitting and Evaluation

The model is fitted by training the model on the given data to predict the target value. The performance is evaluated to find the accuracy of the prediction and compare model configurations. Different configurations need to be compared to assess the goodness of fit of the meta-model. For regression, there are five common metrics to evaluate the predictions listed in Equations (4)–(8) below:

- Mean absolute percentage error,

$$MAPE = \frac{100\%}{N} \sum \frac{|y_i - \hat{y}_i|}{y_i} \tag{4}$$

- Mean squared error,

$$MSE = \frac{1}{N} \sum (y_i - \hat{y}_i)^2 \tag{5}$$

- Root mean squared error,

$$RMSE = \sqrt{MSE} \tag{6}$$

- Error,

$$E = (y_i - \hat{y}_i) \tag{7}$$

- Coefficient of determination,

$$R^2 = 1 - \frac{\sum (y_i - \hat{y}_i)^2}{\sum (y_i - \bar{y}_i)^2} \tag{8}$$

where  $y_i$  is the true value,  $\hat{y}_i$  is the predicted value, and  $\bar{y}_i$  is the mean value of the true value.  $N$  is the number of training cases. When a model is built with acceptable performance, it can predict the desired value of future inputs. The model does not need to be trained for each time it is used, and the trained model is the final product, which is the tool that can be utilized for future prediction.

5.4. Selection and Normalisation of Dataset

In this study, an actual 3 h dynamic response is performed on an FPSO platform exposed to an environmental load. Sample parts of the time series that characterize the simulator’s platform motion for each environmental condition are selected. Each part represents a data window and corresponds to a training unit. The data window size is a system parameter and is kept fixed for the ANNs model. Data windows are independent of each other and can be drawn from completely random points within these three-hour data regarding the same environmental condition. Likewise, data windows are sampled from other selected environmental conditions, and the set of all these training units forms a training set for a neural network. A total of 3,446,077 response samples for mooring tension and 13,320 response samples for the platform offset, in various platform working conditions, are applied for neural network training, validation, and testing. The generated FEM data samples for the dataset are assembled as one long sequence, including non-numeric (string) and numeric quantities illustrated in Tables 6 and 7, respectively. The string value features for mooring tension prediction consist of the number of mooring lines, the angle of inclination of the line azimuth, the anchorage radius, and vessel’s draft so that they act like labels to numerical value features in each sample case, making convergence of networks much faster during training and providing more precise tension prediction values while having a new operational condition. For instance, non-numeric values introduce to dataset via one-hot encoding approach. This method involves creating a new binary string for each category in the dataset, with a value of 1 indicating the presence of the category and a value of 0 indicating the absence of the category. All qualitative and quantitative input features in each sample case assemble as one input tensor vector. Furthermore, the normalization technique, widely used for the numerical features in deep learning, speeds up the convergence of the training process when applying the neural network. Normalization means converting floating-point feature values from their natural range into a standard range. Two main types of normalization techniques are used for the numerical features of the dataset. When data are almost uniformly distributed across a fixed positive range, linear scaling normalization is prescribed. While data are in normal distribution and do not contain extreme outliers, Z-score normalization is used. Based on this principle and the obtained FEM data, the numerical features for mooring tension are normalized to the Z-Score. The numerical features for platform offset are normalized to linear scaling as defined in Equations (9) and (10).

**Table 6.** Samples and features of the dataset for predicting the mooring tension. (S) refers to the string value. (D) refers to the double numerical value.

Samples	Number of Lines (No.) (S)	Azimuth Inclination (Deg.) (S)	Anchorage Radius (m) (S)	Draft (m) (S)	Surge (m) (D)	Sway (m) (D)	Heave (m) (D)	Roll (Deg.) (D)	Pitch (Deg.) (D)	Yaw (Deg.) (D)	Tension (kN) (D)
1	20	5	2500	11	1.85	−4.53	4.24	−7.32	−2.82	1.19	3096.62
2	28	5	2500	11	−1.67	2.614	−1.72	1.11	0.73	−0.446	2699.09
•	•	•	•	•	•	•	•	•	•	•	•
•	•	•	•	•	•	•	•	•	•	•	•
•	•	•	•	•	•	•	•	•	•	•	•
3445K	20	2.5	3000	21	2.1	−1.4846	1.121	−1.4753	3.0961	0.3613	2242.47
3446K	28	2.5	3000	21	−1.67	0.6134	−1.7188	1.1088	0.7298	−0.4462	1829.49

**Table 7.** Samples of measured metocean and operational conditions for floater’s offset prediction. Features of the dataset: number of anchor lines, 20; anchorage radius, 3000 m; line azimuth angle 2.5°. All angles are from the true north. (S) refers to the non-numeric string value. (D) refers to the double numerical value.

Test Runs	H <sub>S1</sub> (m) (D)	T <sub>P1</sub> (s) (D)	θ <sub>1</sub> (°) (S)	H <sub>S2</sub> (m) (D)	T <sub>P2</sub> (s) (D)	θ <sub>2</sub> (°) (S)	φ (°) (S)	Draft (m) (S)
1	1.3	4	0	0.6	4.8	90	0–355	11
2	2.1	4.5	45	1	7.7	135	0–355	11
•	•	•	•	•	•	•	•	•
•	•	•	•	•	•	•	•	•
•	•	•	•	•	•	•	•	•
13,319	5.3	17	180	2.2	7.9	90	0–355	21
13,320	9.8	17.5	225	3.1	10.4	135	0–355	21

Z-Score normalization:

$$X_{ANN} = \frac{X_{FEM} - \mu(X_{FEM})}{\sigma(X_{FEM})} \tag{9}$$

Linear scaling normalization:

$$X_{ANN} = \frac{X_{FEM} - (X_{FEM})_{min}}{(X_{FEM})_{max} - (X_{FEM})_{min}} \tag{10}$$

The six-degree-of-freedom platform motions for the whole dataset are illustrated in Figure 12. The model is trained by providing a time series with 6DOF platform motions in 100-s intervals as the input. The time series of the corresponding mooring line tension is also used as the training output of the network with a 50-s interval. A sliding window is applied to both input and output data to limit the complexity of the prediction, speed up convergence, and thus increase the network’s yield. This is because the NARX model was cleverly built through two tapped-delay lines: one sliding over the input vector and the other sliding over the network’s output. This lagged method facilitates the processing of a sequence of data in an efficient and structured way and to extract features from a data sequence while preserving the relationship between adjacent data points [25]. An illustration of how the sliding window is applied is shown in Figure 9.

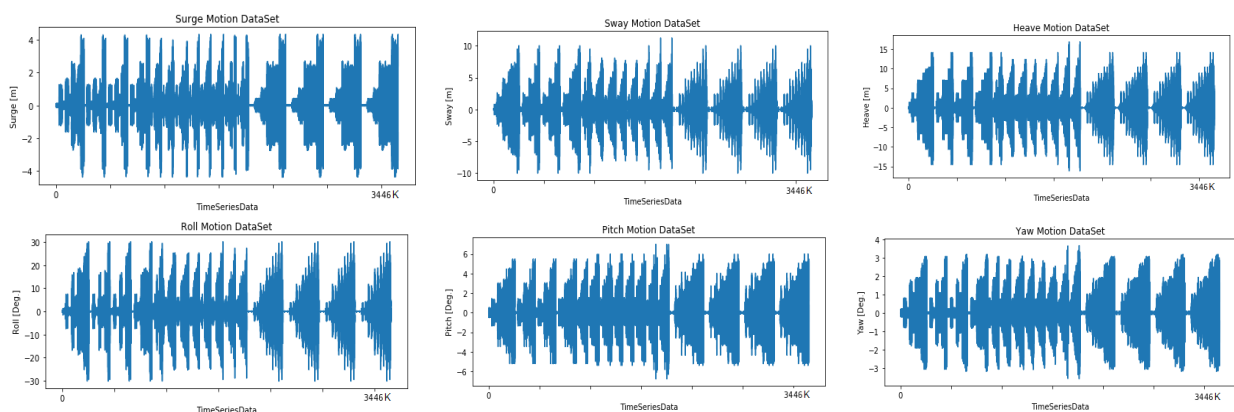


**Figure 12.** FEM dynamic model simulated data: 6DOF platform motion response data visualization.

### 6. Results and Discussion

The figures illustrated in this section are the outcomes of the testing trained network, which were carried out to assess the performance of the proposed models implemented through deep learning. In each subsection, the testing data used for prediction are elaborated in detail, and the results are discussed.

### 6.1. Mooring Tensions Prediction

Simulation data for the model consisting of attributes combinations already mentioned in Table 4 representing several new operating conditions of the floating platform and unseen by the trained model feeding the testing dataset. In total, eight testing units with different time windows were used to predict the anchor line tension. As simulated data are used here, the idea is to provide input data and compare the ANN model output with the simulation, observing the disparity between them. The tension prediction charts for the model's performance testing of the mooring lines are illustrated in Figure 13, in accordance with its defined operational conditions regarding sea state severity, heading direction, draft, anchorage radius, azimuth angle, and number of mooring lines. As can be seen, pattern recognition faces challenges whenever non-linearity increases more than the order of simulated data used for training. Thus, the model cannot capture the testing data points, and prediction accuracy will diminish as the mooring line tension is the corresponding response of a platform's dynamic motions. High non-linearity is associated with low draft, larger line azimuth inclination angle, and smaller anchorage radius. Tension prediction in a very low sea state is also a demanding task since a small environmental load has no major effect on the dynamic motion response of the platform. In this case, the trained model performs poor generalization over the testing subset for prediction. The over-prediction versus under-prediction can be seen since the model was trained by a very severe sea state ( $H_S = 16$  m  $T_P = 17$  s). The extreme values of tension (peaks) and the tension cycles (periods) of each tested case have been observed carefully. The tension peaks and tension cycles are more compatible with the original signals in twenty mooring lines arrangement  $N_1 = 20$ , which is crucial for fatigue analysis. It can also be seen that the correlation of the predicted signal is more sensitive to the number of employed mooring lines and anchorage radius rather than the azimuth inclination angle, draft, heading, and sea state, which stand as the next influential features affecting tension prediction. Generally, higher sea state conditions and larger anchorage radius showed a better correlation among predicted signals. The correlation coefficients between the predicted and actual tension data at full draft (21 m) are also shown in Figure 14. Actually, the accuracy of the neural network for each test case varies considering new combined features and the correlation coefficient  $R^2$  for all experiments, between 0.8 and 0.98, which is evidence of appropriate correlation of the trained model for different operational conditions. Table 8 presents the statistical errors for the prediction results of three case studies, demonstrating higher error metrics and a lower correlation factor when testing the trained model with unseen data. Three case studies were tested by the trained model: lower level, median level, and upper level of anchorage radius (2500 m, 2750 m, 3000 m), draft (11 m, 16 m, 21 m), and anchor line azimuth angle ( $2.5^\circ$ ,  $3.5^\circ$ ,  $5^\circ$ ). The coefficient of determination  $R^2$ , mean absolute percentage error (MAPE), mean absolute error (MAE), root mean square error (RMSE), and maximum tension error (E) were calculated for eight sea state conditions and the corresponding heading directions of each record. The highest error values associated with the lowest correlation belonged to the second case study (median level), while the third case study (upper level) had the highest prediction accuracy. Furthermore, different levels of design attributes influencing the prediction performance have been depicted in Figure 15, an error bar graph for twenty anchor lines arrangement  $N_1 = 20$ . The influence of design features on the response prediction compared to each other, and the absolute error value of the maximum upper and minimum lower limits of the predicted tension (peaks and troughs), have been displayed for each test case. The sea state intensity, sea state heading direction, vessel's draft, anchorage radius, and anchor line azimuth angle were tested with different magnitudes for the mooring line with maximum tension. Testing and evaluation of errors for each case study with predefined levels were accomplished, while other attributes were kept constant. As can be seen, the prediction error for very low sea state ( $H_S = 2$  m), ballast condition (draft = 11 m), anchorage radius  $L_{AR} = 2750$  m, and anchor line azimuth angle  $\theta = 3.5^\circ$  is much higher than other levels. The range of absolute errors for sea state intensity, various heading directions, vessel's draft, anchorage radius, and anchor

line azimuth angle are within the ranges of 1.35–5.5%, 1.3–2.7%, 1.9–4.6%, 2.1–5.7%, and 1.85–4.2%, respectively. It shall be noted that these values are for the mentioned case studies, and any new combination of attributes results in a new testing subset leading to distinctive outcomes.

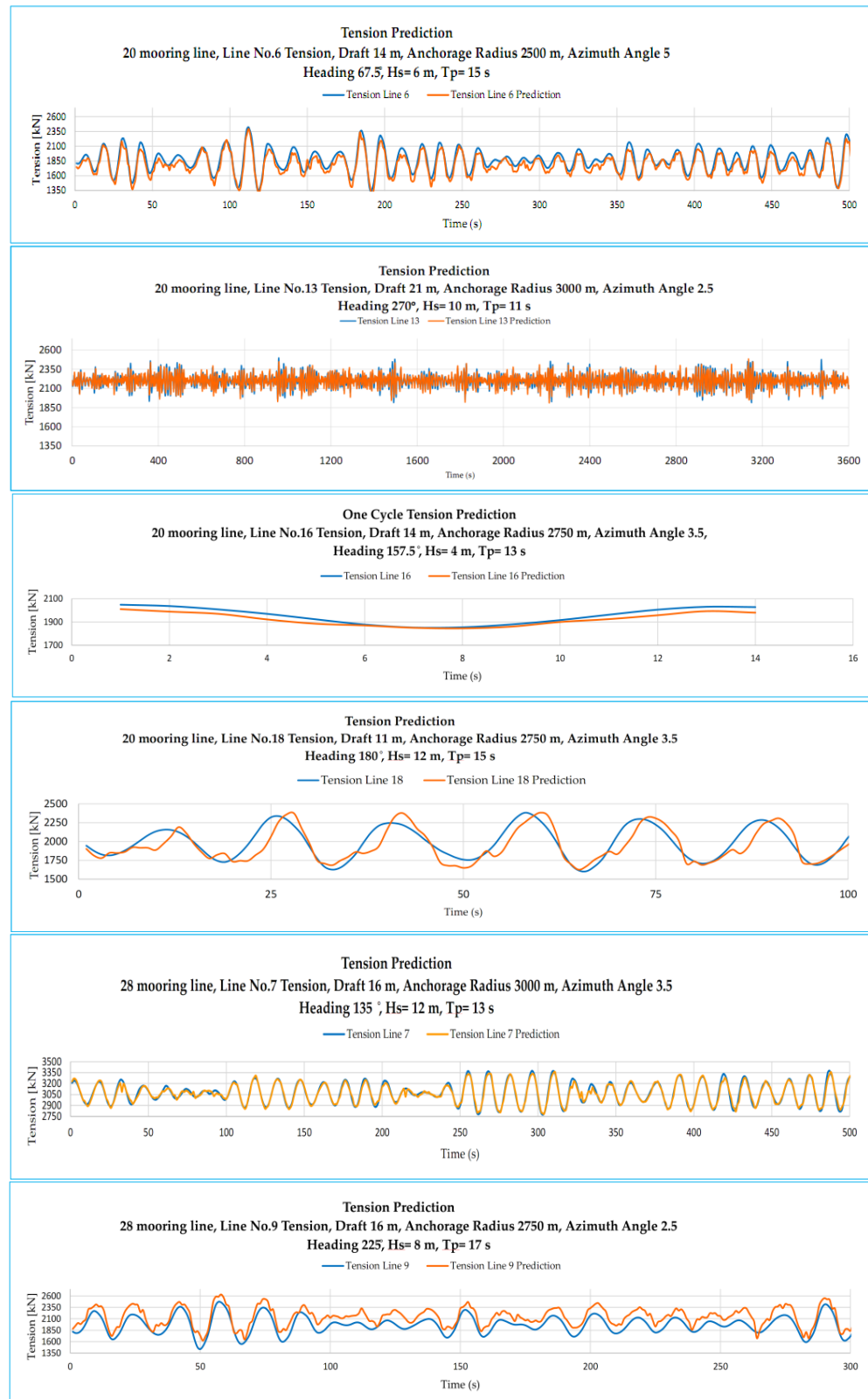


Figure 13. Cont.

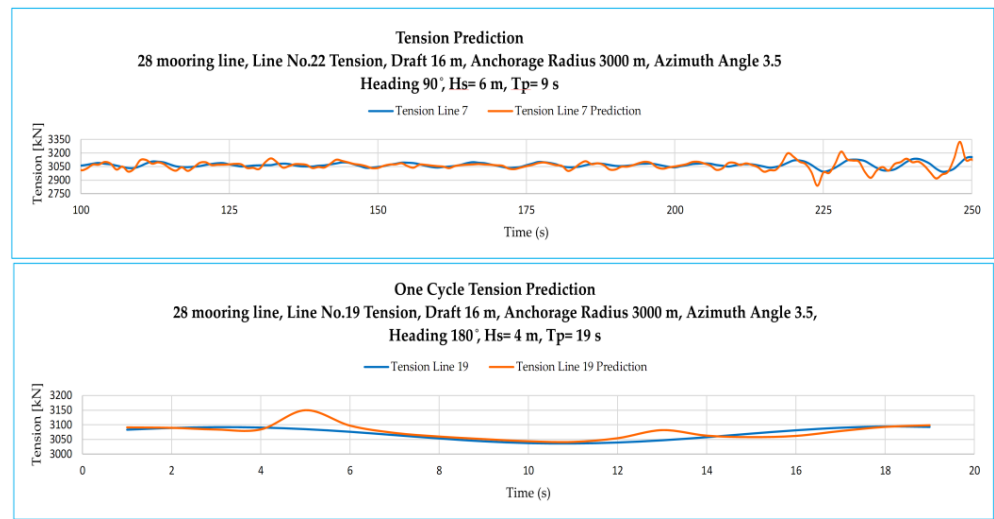


Figure 13. Time series of prediction of mooring line tension versus new working conditions of the platform.

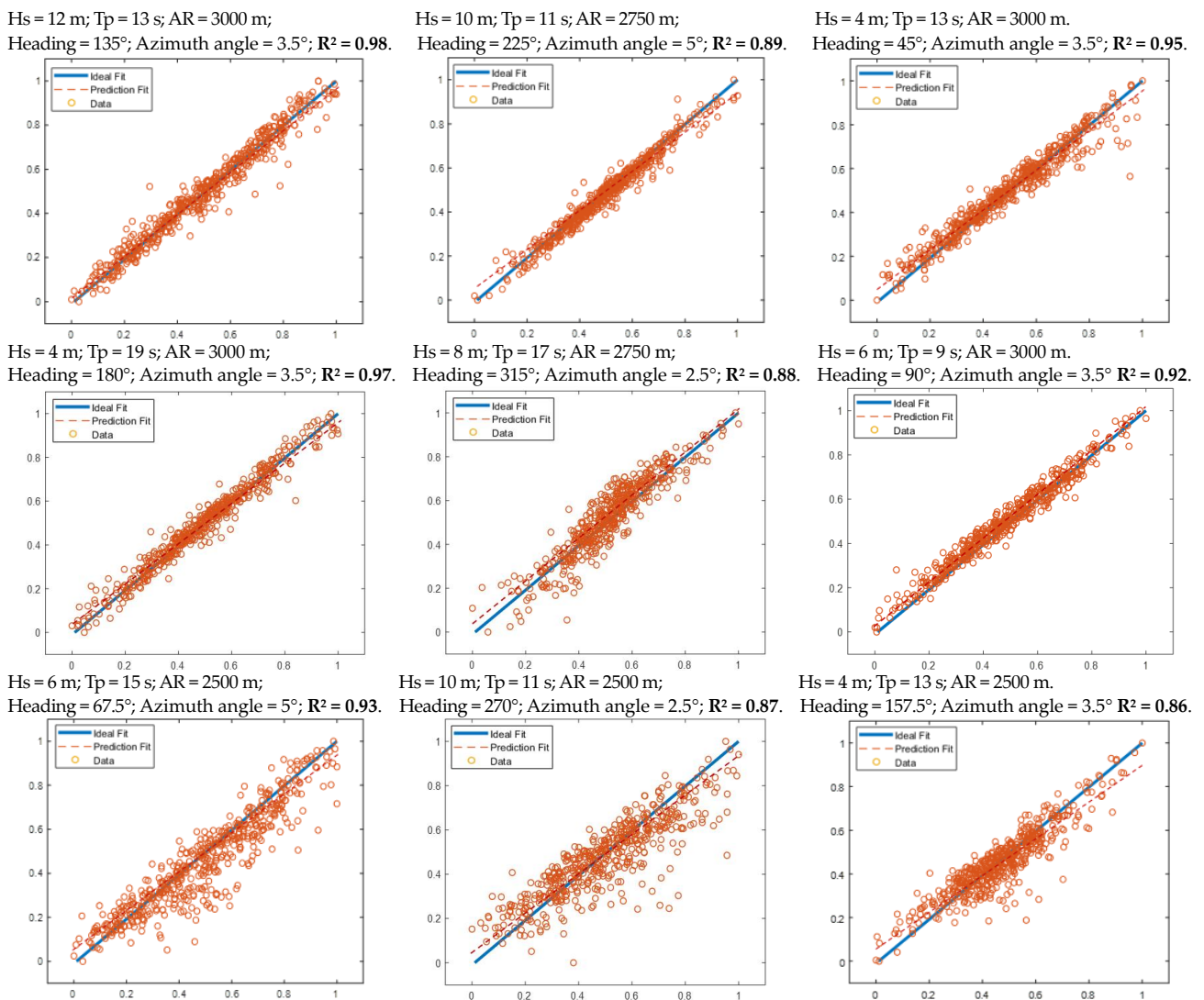
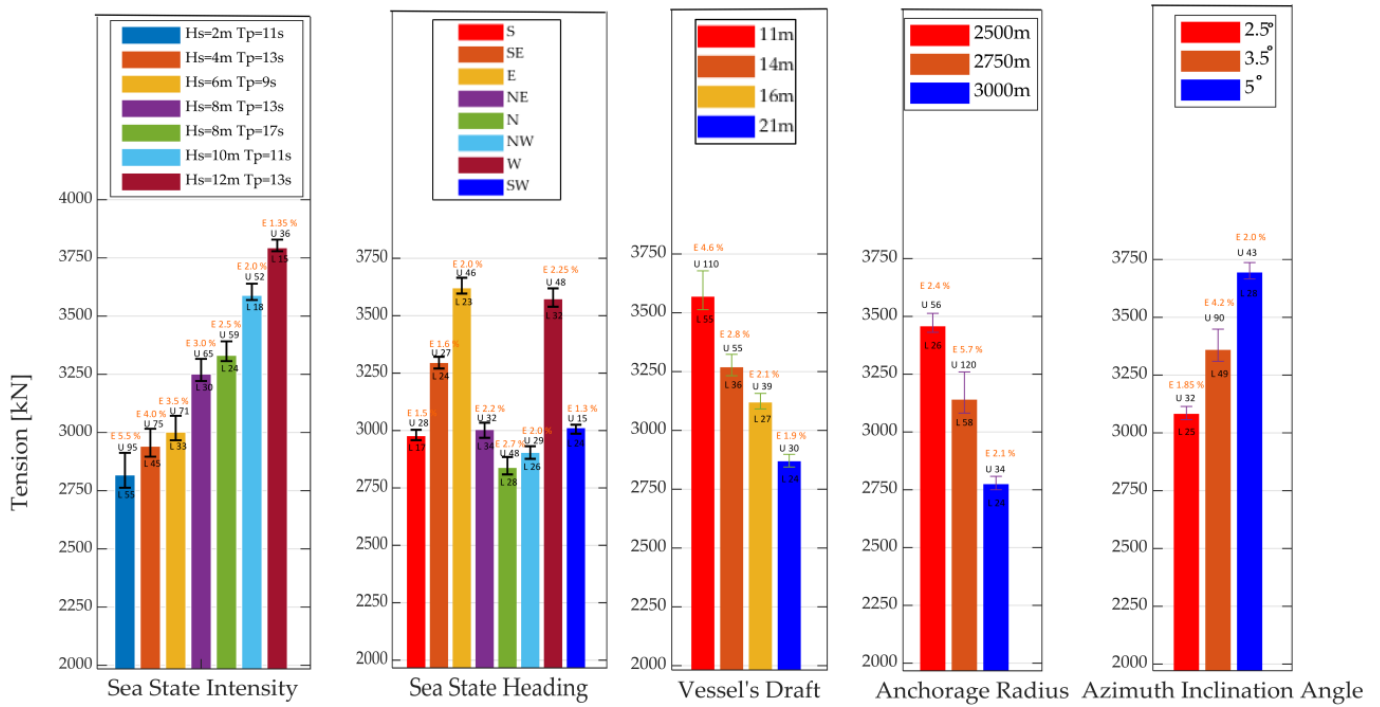


Figure 14. Normalized values from the regression of neural networks for tension prediction at full draft = 21 m.

**Table 8.** Statistical errors for the prediction of tension under various sea states and heading directions.

Variables	H <sub>s</sub> (m)	T <sub>p</sub> (s)	θ (°)	R <sup>2</sup>	MAPE	MAE	RMSE	Ten_FEM (Max.)	Ten_ANN (Max.)	E (%)
<i>L<sub>AR</sub></i> = 2500 m <i>Draft</i> = 11 m <i>θ<sub>AZ</sub></i> = 2.5°	2	11	N	0.924	0.005	15	20	2046	2052	0.2
	4	13	NE	0.954	0.004	12	16	2456	2463	0.2
	6	9	E	0.917	0.006	19	25	2844	2835	0.3
	6	15	SE	0.926	0.005	15	20	3287	3279	0.2
	8	13	S	0.911	0.006	19	25	3517	3527	0.3
	8	17	SW	0.978	0.003	8	11	3507	3512	0.1
	10	11	W	0.877	0.009	25	30	3625	3617	0.2
	12	13	NW	0.985	0.002	6	10	3724	3720	0.1
<i>L<sub>AR</sub></i> = 2750 m <i>Draft</i> = 16 m <i>θ<sub>AZ</sub></i> = 3.5°	2	11	N	0.891	0.0085	27	38	1981	1998	0.8
	4	13	NE	0.899	0.008	25	37	2063	2077	0.6
	6	9	E	0.812	0.019	53	66	2544	2500	1.7
	6	15	SE	0.871	0.012	31	42	3140	3107	1
	8	13	S	0.829	0.018	49	58	3376	3358	0.5
	8	17	SW	0.883	0.011	28	39	3351	3332	0.6
	10	11	W	0.828	0.018	49	58	3453	3484	0.9
	12	13	NW	0.897	0.008	24	25	3567	3539	0.8
<i>L<sub>AR</sub></i> = 3000 m <i>Draft</i> = 21 m <i>θ<sub>AZ</sub></i> = 5°	2	11	N	0.967	0.0035	10	14	1950	1955	0.25
	4	13	NE	0.988	0.0015	4	7	2240	2237	0.1
	6	9	E	0.931	0.0045	13	18	2418	2424	0.2
	6	15	SE	0.989	0.0015	4	6	2826	2828	0.07
	8	13	S	0.974	0.003	8	11	3039	3036	0.1
	8	17	SW	0.981	0.002	6	10	3166	3163	0.09
	10	11	W	0.945	0.004	12	16	3446	3443	0.08
	12	13	NW	0.989	0.0015	4	6	3673	3675	0.05



**Figure 15.** Comparison of prediction error bars for different levels of design attributes tested using the trained model. E (absolute error); U (predicted tension upper limit); L (predicted tension lower limit).

### 6.2. FPSO Offset Chart Prediction

Unlike mooring tension, which is highly dependent on the mooring system and dynamic motion response of the floater to environmental loads, the allowable offset highly depends on the approaching sea state and draft, known as the vertical distance between the waterline and the bottom of the hull, also known as the keel. The dynamic response to incident metocean conditions is highly dependent on its draft, as it is related to the structural properties of the vessel, such as its mass, metacentric height, and the position of its center of gravity (CG). Therefore, the feature selection for offset predictive models must account for the draft's influence, as well as the intensity of the sea state ( $H_S$ ,  $T_P$ ) and the incident heading direction. As a first approximation, the offset is defined as the maximum displacement of the center of gravity in each direction ( $X$  and  $Y$ , respectively) when under environmental loads, as illustrated in Figure 16. The maximum allowable offset is then computed as a summation of the maximum displacements of the platform in the  $X$  and  $Y$  direction, which is finally defined as Equation (11):

$$R^2 = X_G^2 + Y_G^2 \tag{11}$$

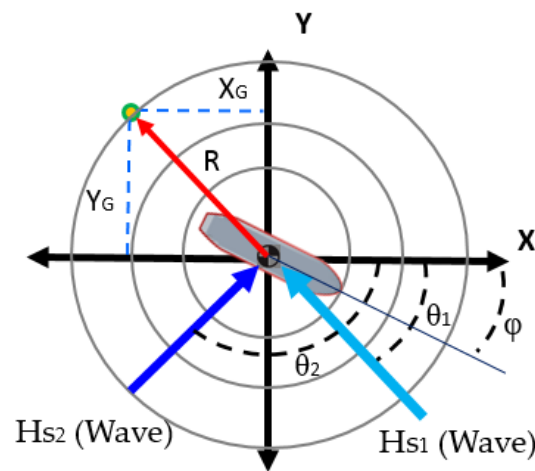


**Figure 16.** Visualization of environmental condition projection for offset ( $R$ ) calculation and prediction ( $R^2 = X_G^2 + Y_G^2$ ).

There is a high percentage of double-peak wave spectra at the Santos Basin because of sea conditions associated with local blowing winds and swell conditions associated with southern extratropical cyclones. These spectra are usually characterized by a peak associated with the sea component with a frequency higher than 0.1 Hz and a peak associated with the swell component with a frequency lower than 0.1 Hz. Under some conditions, one of these peaks may be associated with a local storm that generates an extreme double-peak wave condition called the extreme double-peak wave criteria [22]. The extreme curves of the first spectral peak ( $H_{S1}$ ,  $T_{P1}$ ) and associated second spectral peak ( $H_{S2}$ ,  $T_{P2}$ ) for some double-peak sea states are presented in Figure 17, where the directions of both primary and secondary components are separated by a right angle ( $90^\circ$ ). These situations can affect the motion of units that may be aligned with one of these directions. It is only possible to calculate double-peak curves that have directions associated with existing local meteorological and oceanographic conditions. Thus, it is not possible to calculate curves for sixteen directions as performed for single-peak extreme sea states. The dataset selection for the platform offset, as depicted in Figure 7, includes the sea state ( $H_{S1}$ ,  $T_{P1}$ ,  $H_{S2}$ ,  $T_{P2}$ ), the vessel's draft, and the heading direction ( $\varphi$ ) toward the approaching sea state as key factors. Therefore, only these main attributes are considered for the generation of data and offset prediction, while other relevant factors remain constant. There are 185 sea state cases with first spectral peak ( $H_{S1}$ ,  $T_{P1}$ ) and associated second spectral peak ( $H_{S2}$ ,  $T_{P2}$ ) that have been tested for 36 heading directions. In total, 13,320 test runs were considered for

the generation as illustrated in Table 7. The 1998 sample cases for all defined sea states and heading directions were selected for testing dataset and platform offset prediction. Except for the number of neurons in each layer and activation function between hidden layers, all other hyperparameters of this network are the same as the ones already defined in Table 5. A rectified linear unit (ReLU) as an activation function, which introduces the property of non-linearity to a deep learning model and solves the vanishing gradients issue, is being applied to hidden neurons of this network. The model results include platform offset prediction and the colormap of the prediction error plotted in Figure 18. The predicted values are plotted in three polar diagrams to determine the maximum offset in each direction and the loading condition of the platform. As expected, the effect of the vessel's draft and heading direction is reflected in the maximum offset and highest absolute error. The light draft resulted in larger displacement, while the platform was subjected to the same environmental loads as the heavy draft. The prediction error is also within an acceptable range for almost all metocean conditions and heading directions tested. The error spikes vary between 0.7 m and 1 m for two conditions, indicating that the model error is larger for light draft than for heavy draft, specifically in low sea state conditions.

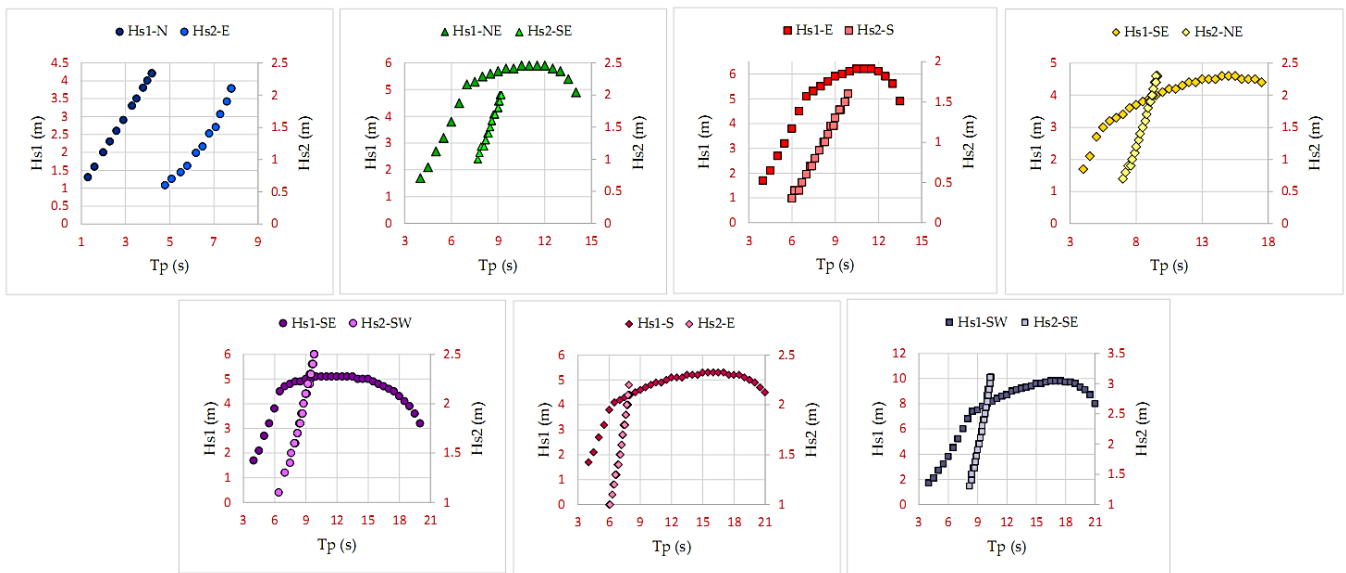


Figure 17. Metocean data for extreme double-peak wave criteria of Santos basin offshore Brazil [22].

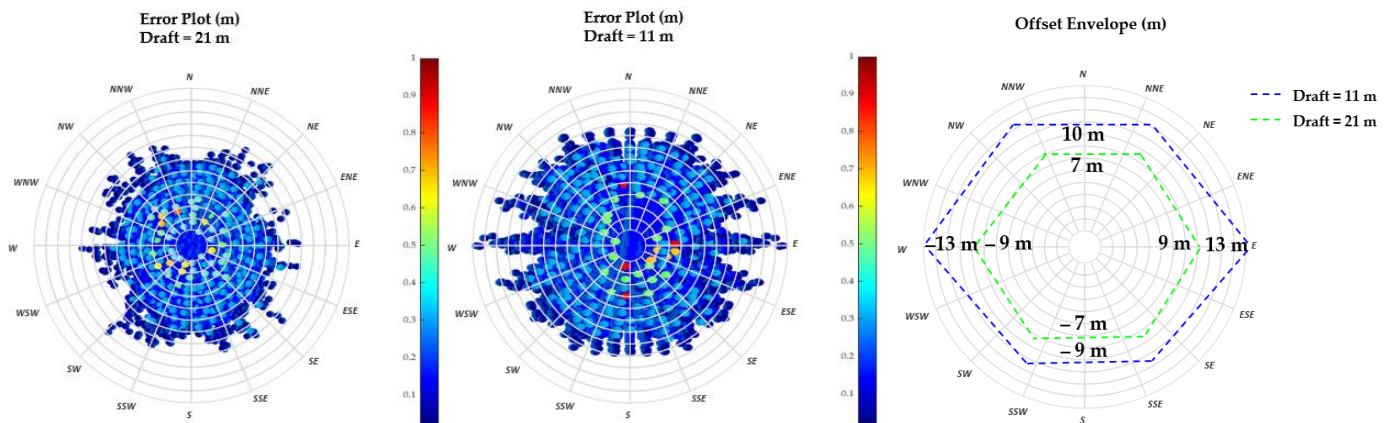


Figure 18. Error plots of the offset chart and envelope prediction for extreme double-peak wave criteria.

### 6.3. Discussion

The trained model for tension time series prediction was tested with simulated data, generated via an FEM numerical model, relevant to various operational characteristics of the floating platform and metocean data of the target offshore field, as already defined in previous sections. It was tested with data not used yet by the model to observe the correlation and maximum error of the predicted data points and signals. The combinations of two different arrangements of mooring lines ( $N_1 = 20$  and  $N_2 = 28$ ), three lengths of anchorage radius ( $L_{AR} = 2500$  m,  $L_{AR} = 2750$  m,  $L_{AR} = 3000$  m), four drafts ( $D_1 = 11$  m,  $D_2 = 14$  m,  $D_3 = 16$  m,  $D_4 = 21$  m), and three azimuth inclination angles ( $\theta = 2.5^\circ$ ,  $\theta = 3.5^\circ$ ,  $\theta = 5^\circ$ ), along with all the sea states and heading directions mentioned in Table 4, were utilized to generate data for testing. As explained in the context of this section, for all experiments, the error decreases when the model experiences sufficient similar training samples as the testing ones. The model will avoid poor generalization issues while dealing with unseen sample cases. Generally, increasing the number of anchor mooring lines challenges the model prediction for mooring tension. Tension time series prediction for twenty anchor lines arrangement  $N_1 = 20$  had a higher correlation among all testing cases than twenty-eight anchor lines framework  $N_2 = 28$ . It experienced peaks and troughs that exceeded the original signal in lower and upper limits. The lower limit of the tension prediction among all defined features varied from  $T_{Lower\ Limit} = 17$  kN to  $T_{Lower\ Limit} = 58$  kN, while the upper limit varied from  $T_{Upper\ Limit} = 15$  kN to  $T_{Upper\ Limit} = 120$  kN, as illustrated in Figure 15. The worst-case condition for prediction performance, confronting the highest error, belonged to the combination of low sea state, low draft, quartering to beam sea heading,  $L_{AR} = 2750$  m anchorage radius, and  $\theta = 3.5^\circ$  azimuth inclination angle. However, the optimum test case sample for tension prediction included the combination of high sea level, maximum draft, heading direction of the head sea,  $L_{AR} = 3000$  m anchorage radius and  $\theta = 2.5^\circ$  azimuth inclination angle. The coefficient of determination  $R^2$ , mean absolute percentage error (MAPE), mean absolute error (MAE), root mean square error (RMSE), and maximum tension error (E) were obtained for tension prediction throughout the combinations of design attributes. The magnitudes of statistical metric errors had fair values, proving the accuracy improvement with the implemented method. They included the following:  $R^2 = 0.8$ – $0.98$ ,  $MAPE \approx 0.0015$ – $0.019$ ,  $MAE \approx 6$ – $53$  kN,  $RMSE \approx 6$ – $66$  kN,  $E \approx 1.3$ – $5.7\%$ .

The same strategy was implemented to test the platform offset. The accuracy of prediction greatly depends on the platform heading toward the sea state, and its loading condition. The maximum absolute error for offset prediction for draft  $D = 11$  m was between 0.7 and 1.0 m in low to high sea states from S to N. Indeed, it greatly depends on the data used for simulation and sample cases which comprises the initial design characteristics of FPSO case study that generated the dataset for training and testing.

## 7. Conclusions

This paper outlines how deep learning can be used to monitor the integrity of a floating platform and its connected mooring system. This analysis looks into the feasibility of predictive surrogate models for a taut-leg moored FPSO platform operating in the offshore Santos Basin in Brazil. The models were based on the DOE method as an alternative to the conventional measuring methods. Supervised feature selection was introduced as a practical method to evaluate the effectiveness of design attributes (inputs), influencing the output for faster convergence of deep learning. The DOE-based test runs were used for data generation from a numerical model that includes a combination of design attributes representing various platform working scenarios. The numerical model was built using the Orcaflex<sup>®</sup> 11.0b software package, which was fed with metocean data from the target offshore site, and the output of the simulation software was the 6DOF motion of the FPSO, mooring lines tension, and platform maximum offset, considering different operational scenarios regarding sea state intensity, various configuration of the mooring system, and platform loading conditions. These generated FEM sample responses were assembled as

one long sequence dataset that included non-numeric (string) and numerical feature values to provide input to two completely distinct networks. The first network was a dynamic deep feedforward NARX MLP with backpropagation of error and developed to predict 50 s mooring line tension time series using a 100 s previous platform motions. The input to the network was simulated data, including the 6DOF platform and its corresponding labeled data, such as the vessel's draft, anchorage radius, number of anchor mooring lines, and azimuth inclination angle indicating the operating conditions of the platform. The second network was a static deep feedforward MLP and employed to predict the platform maximum offset in different heading directions. Inputs to this network were the first and associated second extreme double-spectral peak wave condition ( $H_{S1}$ ,  $T_{P1}$ ,  $H_{S2}$ ,  $T_{P2}$ ), the vessel's draft, and its heading direction. Different portions of these two datasets are selected for training, validation, and testing purposes. Due to the complex dynamic nature and larger structure, the time required for convergence is higher for the first network. Hyperparameter tuning of these two networks, such as setting the number of neurons in each layer and adjusting the activation function, differ from each other due to consistency with the problem-solving strategy. For instance, the dynamic NARX network had more neurons than the static MLP, which made it computationally expensive. Moreover, the Sigmoid activation function performs expensive exponential operations, while ReLU only needs to pick  $\max(0, x)$ . As a final remark, these models are statistics simulation tools to predict and record the tension of the anchor mooring lines and offset chart of the FPSO platform in different working scenarios from low to high sea conditions with acceptable accuracy. The advantage of this methodology is to consider relevant features that are mutually dependent and represent platform working conditions in each sample case, making convergence of ANNs much faster during training. Additionally, ship sensors such as DGPS, DMS, and MOS can easily measure these features to fill out the testing dataset. Observed error spikes for mooring tension prediction, indicating the model error is due to insufficient similar training samples and the resulting generalization issues in these regions. The main drawback of these ANN surrogate models is that they cannot stand alone. To achieve a prediction with high accuracy, they need time-consuming simulations and data generation of the numerical model to provide a proper and refined data window for training, which might consider all possible working scenarios of the floating platform. This problem can be promptly solved if the data used for training the ANNs model are already acquired by ship sensors via long-term monitoring of real FPSO platforms in operation associated with various working conditions. Since the prediction of mooring line tension and floating platform offset in various working conditions sets relevant requirements on the offshore oil and gas industry, the current research presents a promising approach for solving nonlinear problems in this field of study.

**Author Contributions:** E.N.: methodology, software, validation, research and investigation, writing—original draft, writing—review and editing, visualization. A.C.F.: conceptualization, methodology, resources, writing—review and editing, supervision, project administration, funding acquisition. J.-D.C.: formal analysis, writing—review and editing, funding acquisition. All authors have read and agreed to the published version of the manuscript.

**Funding:** Ehsan Nikkhah's work was sponsored by ANP (Brazil's National Oil, Natural Gas and Biofuels Agency), program PHR-7. The authors thank "Laboratório de Ondas e Correntes"; LOC/COPPE/UFRJ, and CNPq (Brazil National Council for Scientific and Technological Development) grant number 309238/2020, and the Brazilian National Council for the Improvement of Higher Education (CAPES) for financial and technical support.

**Institutional Review Board Statement:** This study was approved by the Institutional Review Board (IRB) of Federal University of Rio de Janeiro, Brazil.

**Informed Consent Statement:** Not applicable.

**Data Availability Statement:** The data that support the findings of this study are available from the corresponding author upon reasonable request.

**Conflicts of Interest:** The authors declare no conflict of interest.

## References

- Banfield, S.; Casey, N. Evaluation of Fibre Rope Properties for Offshore Mooring. *Ocean Eng.* **1998**, *25*, 861–879. [CrossRef]
- Ma, K.-T.; Luo, Y.; Wu, Y. *Mooring System Engineering for Offshore Structures*; Elsevier: Amsterdam, The Netherlands, 2019; pp. 85–114. [CrossRef]
- Domingos, P. A few useful things to know about machine learning. *Commun. ACM* **2012**, *55*, 78–87. [CrossRef]
- Godoy Simoes, M.; Leonidas Merma Tiquilloca, J.; Mitio Morishita, H. Neural-network-based prediction of mooring forces in floating production storage and offloading systems. *IEEE Access* **2002**, *38*, 457–466. [CrossRef]
- Guarize, R.; Matos, N.A.F.; Sagrilo, L.V.S. Neural networks in the dynamic response analysis of slender marine structures. *Appl. Ocean. Res.* **2007**, *29*, 191–198. [CrossRef]
- Christiansen, N.H.; Torbergsen Voie, P.E.; Høgsberg, J.; Sødahl, N. Efficient Mooring Line Fatigue Analysis Using a Hybrid Method Time Domain Simulation Scheme. *OMAE* **2013**, *1*, T01A035. [CrossRef]
- De Pina, A.C.; De Pina, A.A.; Albrecht, C.H.; De Lima, B.S.; Jacob, B.P. ANN-based surrogate models for the analysis of mooring lines and risers. *Appl. Ocean. Res.* **2013**, *41*, 76–86. [CrossRef]
- De Pina, A.C.; De Pina, A.A.; Albrecht, C.H.; De Lima, B.S.; Jacob, B.P. Wavelet network meta-models for the analysis of slender offshore structures. *Eng. Struct.* **2014**, *68*, 71–84. [CrossRef]
- De Pina, A.C.; De Pina, A.A.; Albrecht, C.H.; De Lima, B.S.; Jacob, B.P. Artificial Neural Networks for the analysis of spread mooring configurations for floating production systems. *Appl. Ocean. Res.* **2016**, *59*, 254–264. [CrossRef]
- Sidarta, D.E.; Kyoung, J.; O’Sullivan, J.; Lambrakos, K.F. Prediction of Offshore Platform Mooring Line Tensions Using Artificial Neural Network. *OMAE* **2017**, *1*, T01A079. [CrossRef]
- Yetkin, M.; Kim, Y. Time series prediction of mooring line top tension by the NARX and Volterra model. *Appl. Ocean. Res.* **2019**, *88*, 170–186. [CrossRef]
- Zhao, Y.; Dong, S.; Jiang, F. Reliability analysis of mooring lines for floating structures using ANN-BN inference. *J. Eng. Marit. Environ.* **2020**, *235*, 236–254. [CrossRef]
- Zhao, Y.; Dong, S.; Jiang, F.; Incecik, A. Mooring tension prediction based on BP neural network for semisubmersible platform. *Ocean Eng.* **2021**, *223*, 108714. [CrossRef]
- Lee, D.; Lee, S.; Lee, J. Standardization in building an ANN-based mooring line top tension prediction system. *Int. J. Nav. Archit. Ocean. Eng.* **2022**, *14*, 100421. [CrossRef]
- Cotrim, L.P.; Barreira, R.A.; Santos Ismael, H.F.; Gomi, E.S.; Reali Co, A.H. Neural Network Meta-Models for FPSO Motion Prediction from Environmental Data With Different Platform Loads. *IEEE Access* **2022**, *10*, 86558–86577. [CrossRef]
- Li, P.; Jin, C.; Ma, G. Evaluation of Dynamic Tensions of Single Point Mooring System under Random Waves with Artificial Neural Network. *J. Mar. Sci. Eng.* **2022**, *10*, 666. [CrossRef]
- Lopez, J.T.; Tao, L.; Xiao, L.; Hu, Z. Experimental study on the hydrodynamic behavior of an FPSO in a deep water region of the Gulf of Mexico. *J. Ocean. Eng. Technol.* **2017**, *129*, 549–566. [CrossRef]
- DNVGL-RP-F205; Global Performance Analysis of Deep-water Floating Structures. Det Norske Veritas & Germanischer Lloyd (DNVGL): Oslo, Norway, 2020; pp. 7–28.
- Petrobras FPSOs Technical Specification. FPSO BRASIL: PETROBRAS P-52; PETROBRAS P-54; PETROBRAS P-55; PETROBRAS P-62. Available online: <https://www.gov.br/ibama/pt-br> (accessed on 12 February 2023).
- Montgomery, D.C. *Design and Analysis of Experiments*, 3rd ed.; Wiley: Hoboken, NJ, USA, 1991; Volume 22, Chapters 5–9; pp. 233–292. [CrossRef]
- Chakrabarti, S.K. *Handbook of Offshore Engineering*; Elsevier Science: Amsterdam, The Netherlands; Offshore Structural Analysis, Inc.: Plainfield, IL, USA, 2005; Volume 2.
- Metoccean Data. Santos Basin Oil Export Studies. Santos Basin Central Cluster Region. *Metoccean Design Criteria. Technical Note and Specification*. Available online: <https://www.scribd.com/document/405828089/Metoccean-Data-pdf> (accessed on 15 March 2023).
- Aizenberg, I.; Aizenberg, N.N.; Vandewalle, J.P.L. *Multi-Valued and Universal Binary Neurons: Theory, Learning and Applications*; First Work to Introduce the Term “Deep Learning” to Neural Networks; Springer Science & Business Media: Berlin/Heidelberg, Germany, 2000.
- Schmidhuber, J. Deep Learning in neural networks: An overview. *Neural Netw.* **2015**, *61*, 85–117. [CrossRef] [PubMed]
- Menezes, J.M.P.; Barreto, G.A. Long-term time series prediction with the NARX network: An empirical evaluation. *Neurocomputing* **2008**, *71*, 3335–3343. [CrossRef]
- Rampasek, L.; Goldenberg, A. TensorFlow: Biology’s Gateway to Deep Learning? *CellSystems* **2016**, *2*, 12–14. [CrossRef] [PubMed]
- López, O.A.M.; López, A.M.; Crossa, J. *Multivariate Statistical Machine Learning Methods for Genomic Prediction*; Springer: Gewerbestrasse, Switzerland, 2022; Volume 1, Chapter 10; pp. 379–425. [CrossRef]

**Disclaimer/Publisher’s Note:** The statements, opinions and data contained in all publications are solely those of the individual author(s) and contributor(s) and not of MDPI and/or the editor(s). MDPI and/or the editor(s) disclaim responsibility for any injury to people or property resulting from any ideas, methods, instructions or products referred to in the content.